Rock and Soil Mechanics

Volume 41 | Issue 7 Article 3

12-22-2020

Study on bearing behavior of flexible single pile subject to horizontal and uplift combined load

Lei ZHANG
Shaanxi Key Laboratory of Geotechnical and Underground Space Engineering, Xi'an University of Architecture & Technology, Xi'an, Shaanxi 710055, China

Wei-shen HAI
Shaanxi Key Laboratory of Geotechnical and Underground Space Engineering, Xi'an University of Architecture & Technology, Xi'an, Shaanxi 710055, China

Hao GAN
Shaanxi Key Laboratory of Geotechnical and Underground Space Engineering, Xi'an University of Architecture & Technology, Xi'an, Shaanxi 710055, China

Wei-ping CAO
Shaanxi Key Laboratory of Geotechnical and Underground Space Engineering, Xi'an University of Architecture & Technology, Xi'an, Shaanxi 710055, China

See next page for additional authors

Custom Citation

ZHANG Lei, HAI Wei-shen, GAN Hao, CAO Wei-ping, WANG Tie-hang, . Study on bearing behavior of flexible single pile subject to horizontal and uplift combined load[J]. Rock and Soil Mechanics, 2020, 41(7): 2261-2270.

Study on bearing behavior of flexible single pile subject to horizontal and uplift combined load

Authors

Lei ZHANG, Wei-shen HAI, Hao GAN, Wei-ping CAO, and Tie-hang WANG

Rock and Soil Mechanics 2020 41(7): 2261−2270 ISSN 1000−7598
https: //doi.org/10.16285/j.rsm.2019.6522 rocksoilmech.researchcommons.org/journal

Study on bearing behavior of flexible single pile subject to horizontal and uplift combined load

ZHANG Lei[1, 2], HAI Wei-shen[1, 2], GAN Hao[1, 2], CAO Wei-ping[1, 2], WANG Tie-hang[1, 2]

1. School of Civil Engineering, Xi'an University of Architecture & Technology, Xi'an, Shaanxi 710055, China

2. Shaanxi Key Laboratory of Geotechnical and Underground Space Engineering, Xi'an University of Architecture & Technology, Xi'an, Shaanxi 710055, China

Abstract: In order to study the bearing behavior of a flexible single pile under combined horizontal and uplift loading, two groups of structural testing, comprised of 6 pile models in total have been carried out. The results show that for a flexible single pile, pre-applied uplift load with a magnitude smaller than half of pure uplifting capacity(Tu1) lead to significant improvement of ultimate horizontal bearing capacity, achieving greater horizontal resistance compared to pure ultimate horizontal bearing capacity (Hu1) Additionally, it has been observed that this horizontal bearing capacity increases initially but decreases subsequently under further increasing uplift load. This load increasing results in reduction of bending moment and soil resistance whilst degrades horizontal stiffness, and consequently, the horizontal displacement of pile increases initially but decreases subsequently under resultant effect. The ultimate uplift bearing capacity of a flexible single pile could be improved under pre-applied horizontal loads not exceeding 0.5Hu1, mainly attributed by increasing the average side friction of pile within the distance of 10 times the diameter of pile below the ground surface. This capacity is strengthened under larger horizontal load, and when this load reaches 0.5Hu1, the magnitude is increased by 17.1% compared with Tu1. This behavior could be taken into account with respect to pile design. The precision of test results has been verified by theoretical analysis, and a formula for calculating the ultimate uplift bearing capacity of flexible single pile under combined loads has been proposed. The corresponding analysis results have achieved good agreements with testing data and the error is less than 6%.

Keywords: pile foundations; bearing behavior; model tests; combined loading; soil-pile interaction; loess subgrade

1 Introduction

Pile foundations applied for underground infrastructure, skyscraper and transmission tower usually works under combined horizontal and uplift loads (abbreviated as combined loads)[1], and traditionally, each load is considered separately in calculation of bearing capacity and deformation of pile in the corresponding direction. The internal force of pile body is calculated following the stress superposition theory. However, this method does not perform well in predicting the pile bearing capacity and deformation under combined loads because the coupled effect caused by horizontal and vertical loads have not been considered. Therefore, the research on the bearing behavior of piles under combined loads is necessary.

A number of studies on the bearing behavior of a single pile under inclined tensile loading have been carried out by researchers in this field. Shin et al.[2] and Yang et al.[3] have investigated the ultimate bearing capacity of a single pile in clay via experimental model testing. Ramadan et al.[4–5] have analyzed and compared bending moment, earth pressure and horizontal displacement along a single pile under pullout load at different inclined angles, and significant interaction between uplift and horizontal loads has been revealed. Some diagrams of this interaction between both components of inclined loading have been plotted by Bhardwaj and Singh[6] and Achmus and Thieken[7]. On the basis of theoretical analysis and testing results, Meyerhof[8] has interpreted the formula of ultimate bearing capacity of rigid pile under inclined loading, and presented corresponding equations explaining the interaction between horizontal and vertical components. The above studies have mainly focused on ideally synchronous and proportional loading in horizontal and vertical directions of single pile. However, in engineering practice, in some structures such as anti-floating and anti-sliding composite pile applied in pumping stations[9], the uplift loads such as buoyancy and frozen-pullout force occur after horizontal loads. Similarly, the uplift pile for high voltage transmission line tower could be subjected to horizontal load caused by earthquake or wind load. Some research has been carried out to study these cases under non-synchronous loading. Rao et al.[10] has investigated the influence of horizontal cyclic loading on uplift ultimate bearing capacity of a rigid pile in clay via experimental model testing, demonstrating that when the horizontal cyclic load is greater than 30% of the static horizontal ultimate

Received: 3 September 2019 Revised: 31 December 2019
This work was supported by the National Natural Science Foundation of China (51508455) and the Fundamental Research Project of Natural Science Foundation of Shaanxi (2019JM-232).
First author: ZHANG Lei, male, born in 1981, PhD, Lecturer, mainly engaged in research on soil-structure interaction. E-mail: zh888lei@163.com

bearing capacity, the uplift ultimate bearing capacity of a single pile is reduced. Luo et al.[11] discussed the influence of uplift load on the horizontal bearing capacity and deformation of a single pile via field testing, and the results have shown a key role of uplift load in reducing soil strength around the pile and increasing soil horizontal displacement under the large horizontal load. Results of model tests given by Reddy et al. [12] have shown that for a single pile, the horizontal bearing capacity increases with increasing pre-applied uplift load, and similarly, the pre-applied horizontal load enhances the uplift bearing capacity. The experimental results also indicated that the significant increase in displacement may limit the application of the pre-applied horizontal and uplift loads in practice. In the discussion of the above study, Schmertmann[13] has given the calculation formula of uplift bearing capacity of a rigid pile under combined loads. Bhavik et al.[14] have come to similar conclusions to those of Reddy et al. [12] from model testing on pile groups.

Limited research on the bearing characteristics of a single pile under unsynchronized combined loads has been carried out in the literature. The bearing capacity is still the major focus in this field whilst existing conclusions are inconsistent. This study has carried out a model test to further investigate the influence of the pre-applied uplift load on bending moment, earth pressure and horizontal displacement of a single pile under lateral load. The study on the influence of the horizontal load on vertical displacement and lateral friction resistance of the uplift loaded pile has also been involved. Theoretical analysis has been performed to verify the obtained testing results, and a set of calculation formula of the uplift ultimate bearing capacity of a flexible single pile under combined loads has been given.

2 Overview of model test

2.1 Model pile

Referring to the concrete pile with a diameter of 0.8 m and 24 m in length, the ratio of scale modelling in this research was determined as 20, following the principle of similarity. The model pile was made of PVC pipe with an outer diameter of 40mm and a wall thickness of 2 mm. The model pile had a length of 1.3 m and was buried at the depth of 1.2 m. The manufacturing process of the model pile has been detailed in the literature[15]. The strain gauge was quarterly bridged, and the bonding position is shown in Fig.1(a). A metal pipe was installed on the cantilever section for loading, and the load was applied at the position 7.5 cm above the ground. A 24.0 cm×10.0 cm×0.5 cm (length× width× thickness) glass plate was stuck on the pile top, where a dial indicator was placed to measure the vertical displacement at this position. Coordinates of measuring points could be read from the attached graph paper, of which pile axis passed the origin. Some mechanical properties of the model pile had been characterized using the simple supported beam method: the average elastic modulus $E = 3.018$ GPa and its corresponding elastic modulus similarity ratio C_E =10; the inertia moment similarity ratio C_I =4.627×10^4; and the bending stiffness similarity ratio C_{EI} =4.648×10^6. As shown in Fig.1, v and θ are the vertical displacement and rotation angle of pile top, respectively; δ_2 and δ_3 are vertical displacements measured by dial gauges B2 and B3, respectively; x_2', x_2 and x_3', x_3 are two sets of distance from B2 and B3 to the center of the pile top corresponding to before and after loading stages, respectively; u and u' are horizontal displacements measured at ground and at B1, respectively.

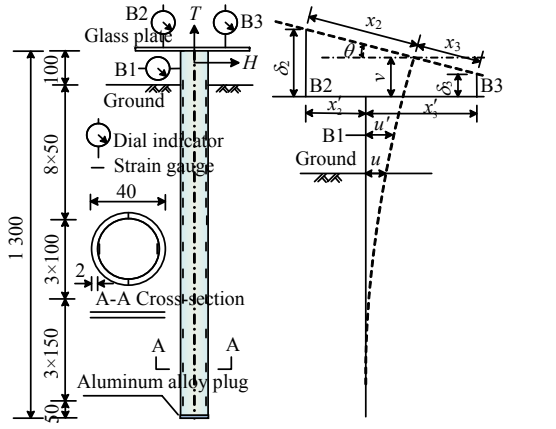

(a) Schematic diagram of model pile instrumentation (b) Schematic diagram of calculation of displacement

Fig. 1 Schematic diagram of pile instrumentation and calculation of displacement (unit: mm)

2.2 Foundation soil

The foundation soil is Pleistocene series aeolian loess sampled from a foundation pit in Beilin, Xiaan at the depth of 6 to 7m below the surface. The relative density of soil particles is 2.72, and the optimal moisture content is 17.65%. The soil has liquid limit and plastic limit of 33.1% and 18.0% respectively, and hence the plasticity index is 15.1. The cohesion of the soil is determined as 23.4 kPa, and the internal friction angle is 26.8°.

Referring to the preparation method of foundation soil introduced by Chandrasekaran et al. [16], the soil sample was dried, crushed and sieved at 2 mm. After fixing the pile in the model box, the remolded soil with optimal moisture content (17.65%) was filled in layers with identical thickness (9 cm) and mass. Each layer was compacted with the same work to remove the redundant air after filling and flattening, ensuring the uniformity of the material. After filling, the upper surface of the soil was covered with a plastic film for

7 days, until the start of the loading test. At the end of the test, an average moisture content of 16.7% and an average dry density of 1.41g/cm^3 were determined for the foundation soil based on the measurement at different depths.

2.3 Test device

(1) Layout of model box and model pile

The model test was carried out in a 1.5 m×0.8 m×2.9 m (length×width×height) model box. The box outer frame is made of welded angle steel, while the 12mm-thick transparent tempered glass was placed at the inner wall for observation. The distance between pile and pile, and that between pile and glass wall in the horizontal loading direction were both 375 mm (>9*D*), while the value of these in the direction of vertical loading were 270mm and 260 mm (6*D*), respectively. The values of these distances were far greater than 3*D*, and thus the influence of different boundary conditions on testing results could be neglected [16–17]. The pile bottom was 150 mm above the box bottom. The structure of the model box is shown in Fig. 2.

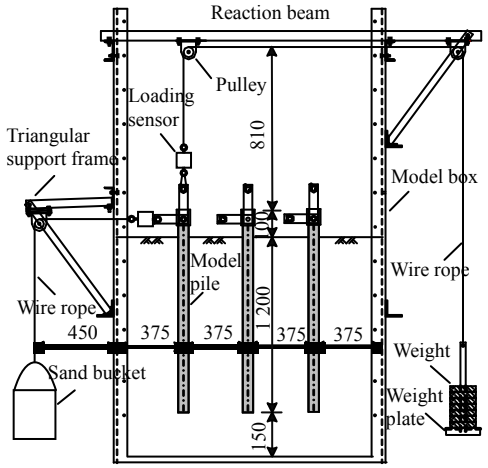

Fig. 2 Schematic diagram of flexible single pile loading test setup (unit: mm)

(2) Loading and measuring device

The loading device included triangular support frame, reaction beam, pile head connecting members, sand buckets and weight plates. The triangular support frame located on the left side of the model box provided reaction force for applying horizontal load. The support frame was protruded outward by 500 mm to increase the distance between the center of the pulley and the left test pile (about 825 mm), and the reaction beam was placed at about 810 mm above the pile top. It was noticed in the test that when the horizontal (or vertical) displacement of loading point reached 15 mm, the steel wire rope connected to the pile body rotated by about 1°, and consequently, the change of vertical (or horizontal) force on the pile top was small. In fact, the maximum displacements of the loading point, either in horizontal (14.7 mm) or vertical (5.9 mm) directions, were lower than 15 mm during the loading process. Therefore, this influence of the loading points displacement on vertical or horizontal forces of the pile top is considered to be negligible. The measurement of load and strain were achieved by a load sensor with a range of 5kN and the CML-1H-32 electronic strain gauge, respectively.

Displacement measurement: as shown in Fig. 1 (b), two dial gauges B2 and B3 with a range of 30 mm were placed on the glass plate located on the pile top to measure the vertical displacement v and rotation angle θ at this position

$$v = \left(\delta_2 x_3 + \delta_3 x_2\right) / \left(x_2 + x_3\right) \tag{1}$$

$$\theta = \arctan\left[\left(\delta_2 - \delta_3\right) / \left(x_2' + x_3'\right)\right] \tag{2}$$

where δ_2 and δ_3 are the vertical displacements measured by B2 and B3, respectively, and the upward direction is specified positive. A dial indicator B1 with a measuring range of 30mm is installed at 50 mm above the ground to measure the horizontal displacement u'. Consequently, the horizontal displacement u of pile at ground could be calculated by the following formula[3]:

$$u = u' - 50 \times \tan\theta \tag{3}$$

2.4 Test scheme

In this paper, two groups of model tests have been introduced, with each involving three pile tests. The first group investigated horizontal bearing characteristics of model piles under pre-applied uplift loads of 0, $T_{u1}/3$ and $T_{u1}/2$, while the other one focused on studying uplift bearing characteristics of model piles under pre-applied horizontal loads of 0, $H_{u1}/3$ and $H_{u1}/2$. The detailed scheme is listed in Table 1.

Table 1 Model test programs

Group	Test pile ID	Uplift load Size	Uplift load Loading mode	Horizontal load Size	Horizontal load Loading mode	Loading sequence
1	P11	0	Constant	H_{u1}	Applied gradually	Uplift-horizontal
	P12	$T_{u1}/3$	Constant	H_{u2}	Applied gradually	
	P13	$T_{u1}/2$	Constant	H_{u3}	Applied gradually	
2	P21	T_{u1}	Applied gradually	0	Constant	Horizontal-uplift
	P22	T_{u2}	Applied gradually	$H_{u1}/3$	Constant	
	P23	T_{u3}	Applied gradually	$H_{u1}/2$	Constant	

The testing was carried out with the slow-continuous loading method. At each increment, the horizontal loading was completed by adding 3.2kg sand into the bucket, while a 15.3kg weight was placed on the weight plate for the uplift loading. Double loading size was adopted for the first stage. The dial indication should be read and recorded immediately after loading, and then the reading was taken every 5 minutes. The loading was considered

to be stable at a single stage when the change of horizontal and vertical displacements was less than 0.01 mm within 10 minutes and that appeared twice in succession [15]. Meanwhile, coordinates of the contact points between the dial indicators (B2 and B3) and the glass plate were read. The next loading stage was carried out after completing collection of the strain of the pile body. The horizontal ultimate bearing capacity of a single pile was determined as the value of the horizontal load applied when the corresponding displacement of the pile at the ground level reached $0.15D$[18]. The uplift ultimate bearing capacity was determined as the uplift load corresponding to the change from curve to straight line section in the curve of uplift load against vertical displacement [19].

3 Results and discussion

3.1 Horizontal bearing characteristics of a single pile

(1) Load−horizontal displacement curve

Figure 3(a) shows curves of horizontal load (H) against displacement (u) of each test pile under uplift loads of 0, T_{u1}/3(815 N) and T_{u1}/2(1 220 N). Continuous growing has been observed in all these three curves. The size of pre-applied uplift loads makes no difference on horizontal displacement of pile body when H is smaller than 300 N. However, at a horizontal force level H larger than 300 N, zero uplift force (pure horizontal loading) leads to the largest displacement, followed by T=T_{u1} /2 and T =T_{u1}/3 in sequence. According to the predicting method of the horizontal ultimate bearing capacity of a single pile described earlier, this horizontal ultimate load could be derived as H_{u1} =590 N、H_{u2} = 725 N and H_{u3} =640 N respectively corresponding to the uplift load of 0, T_{u1}/3(815 N) and T_{u1}/2(1 220 N). H_{u2} and H_{u3} have increased by 22.9% and 8.5% respectively compared with H_{u1}, indicating that the pre-applied uplift load improves horizontal ultimate bearing capacity of a single pile significantly. Specifically, with an increase of uplift load, H_u increases as well at early stage but decreases subsequently, which will be explained later in Section 4.1.

The test pile under pure uplift loading apparently leads to zero horizontal displacement. Figure 3 (b) shows curves of the uplift load (T) against horizontal displacement (u) corresponding to pre-applied horizontal loads of H_{u1}/3(195 N) and H_{u1}/2(295 N). It is evident that for the test pile subject to pre-applied horizontal loads of H_{u1}/3 and H_{u1}/2, the horizontal displacement of pile body at ground increases almost linearly with uplift load. The gradient of curve H= H_{u1}/2 is slightly larger than that of H=H_{u1}/3, indicating that the uplift load applied later is unfavorable to the horizontal deformation resistance of a single pile under horizontal load.

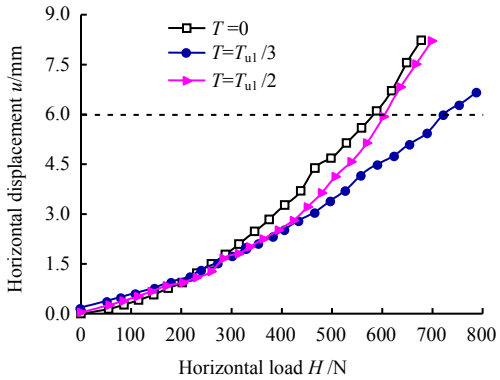

(a) Horizontal load (H)− Horizontal displacement (u) curve

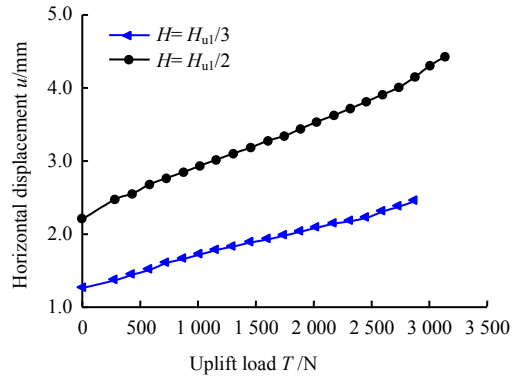

(b) Uplift load (T)− Horizontal displacement (u) curve

Fig. 3 Horizontal deflection of pile at ground against different loads

Figure 3 shows the influence of loading sequence of horizontal and uplift loads on horizontal bearing deformation of a single pile. At a certain level of pre-applied uplift load, the lateral earth pressure on the upper pile is small and develops little friction resistance. Meanwhile, most uplift load has been transferred to the lower foundation, and consequently the horizontal load applied later has no contribution to the friction resistance of the pile section below the effective pile length. In other words, the friction resistance of the pile body within the effective pile length always stays at a small value despite of the increase of horizontal load. Therefore, the unloading effect on the upper soil and the friction effect caused by the friction force on the pile body under these combined loads are very small. It is noted that when horizontal displacement reaches a certain level, the favorable aspect of the second order effect due to displacement (P-Δ effect) will be dominantly effective, which leads to the reduction of horizontal displacement of pile body under pre-applied uplift load. However, the pile under pre-applied horizontal load produces a larger soil reaction force during uplift loading process. It results in an effective increase of the friction resistance of the upper pile body, and thus leads to a greater unloading effect on the upper foundation. In addition, the properties of the upper soil play an important role in the horizontal bearing deformation of

the pile. As the incremental uplift load and horizontal displacement of pile body at each stage are small, the p-Δ effect, deemed favorable in displacement control, is less dominant compared to the adverse effect caused by unloading of the upper foundation. Therefore, applying the uplift load later increases the horizontal displacement of the pile body.

(2) Analysis of internal force and displacement of pile shaft

The measured bending moment M_s of the cross section of the pile shaft could be derived by its bending strain $\Delta\varepsilon$:

$$M_s = EI \cdot \Delta\varepsilon / b_0 = EI(\varepsilon_r - \varepsilon_f)/b_0 \tag{4}$$

where in the same pile section, I is the moment of inertia; b_0 is the distance between two strain gauges; and ε_f and ε_r are the strains in front and rear, respectively. For piles subjected to pure horizontally loading, the real bending moment M at the pile ground under each level of load is the product of the horizontal load and the distance from the force location to the ground (7.5 cm). Figure 4 (a) shows that M_s has a good agreement with M at small horizontal load level, whilst M_s increasingly deviates when the load is growing larger. To guarantee the calculation quality of bending moment along the pile, a principle has been followed, that is, the measured bending moment at the ground level of the pile subjected to pure horizontal load is equal to the actual bending moment. Hence, a formula has been proposed based on regression of data points (see Fig. 4 (b)):

$$M = 1.034M_s - 0.004\ 32M_s^2 \tag{5}$$

The soil reaction force p has been derived via second order (or fourth order) differentiation of functions based on regression over pile bending moment (or displacement) in this research. Some functions commonly implemented for this regression type includes higher-order polynomial, piecewise polynomial, joint function including exponential multiplying polynomial components[20] or exponential multiplying trigonometric components[15]. The exponential-trigonometric joint function shown by the following formula has been employed which yields a higher regression quality.

$$M = a \cdot \exp(-bz^2) \cdot \sin(cz) + d \cdot \exp(-ez^2) \tag{6}$$

where a, b, c, d and e are coefficients determined by calibration; z is the depth below the ground. Therefore, the soil reaction force p is derived as

$$p = -\mathrm{d}^2M/\mathrm{d}z^2 \tag{7}$$

Assuming a linear distribution of bending strain $\Delta\varepsilon$ over adjacent sections, if the pile body is equally divided into n units from bottom to top, the horizontal displacement of pile body at different depths could be calculated using the following formula [21]:

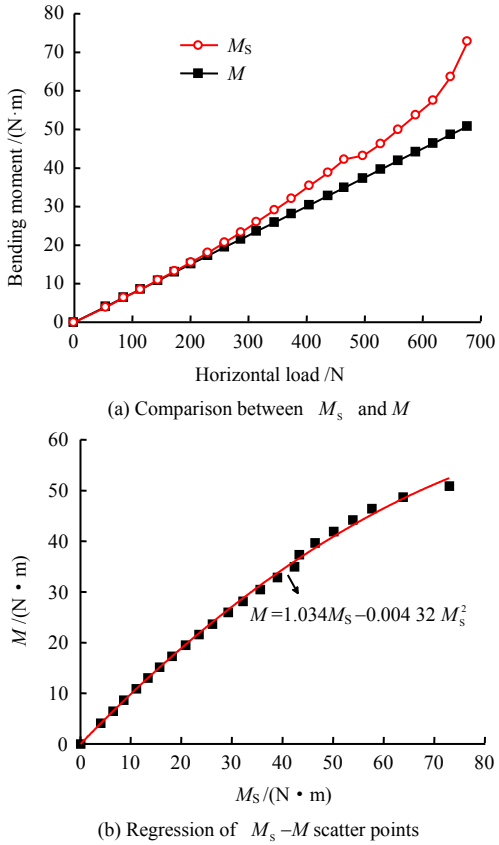

(a) Comparison between M_s and M

(b) Regression of M_s –M scatter points

Fig. 4 Procedure of calibrating bending moment M_s

$$\left.\begin{aligned} y_{i+1} &= y_i + \theta_i l_i + (2\Delta\varepsilon_i + \Delta\varepsilon_{i+1})l_i^2/6b_0 \\ \theta_{i+1} &= \theta_i + (\Delta\varepsilon_{i+1} + \Delta\varepsilon_i)l_i/2b_0 \end{aligned}\right\} \tag{8}$$

where y_i and y_{i+1} are horizontal displacements of cross-sections i and $i+1$, respectively; $\Delta\varepsilon_i$ and $\Delta\varepsilon_{i+1}$ are bending strains of cross-sections i and $i+1$, respectively; θ_i and θ_{i+1} are angles of rotation of cross-sections i and $i+1$, respectively; and l_i is the length of unit i.

Figure 5(a) shows bending moment distribution curves of test piles under pre-applied uplift loads of 0, $T_{u1}/3$ and $T_{u1}/2$, and a horizontal load of 500 N. The comparison among these three curves has revealed that: (1) the pre-applied uplift load dominantly affects the bending moment of the pile body above the first zero-displacement point rather than that of the lower part; (2) compared with the pile subjected to horizontal loading, the pre-applied uplift load significantly reduces the maximum bending moment of the single pile, and the reduction rate decreases with larger uplift load.

Figure 5(b) shows soil reaction force distribution curves of test piles under pre-applied uplift loads of 0, $T_{u1}/3$ and $T_{u1}/2$, and a horizontal load of 500 N. It is noticed that the pre-applied uplift load has little influence on the profile of soil reaction along the pile length, but it reduces the peak value at the first zero-displacement point in upper and lower sections of the pile body. Additionally, with the increase of uplift load, the maximum soil reaction forces of both pile sections have shown a

trend of decreasing.

Figure 5(c) shows horizontal displacement curves of test piles under pre-applied uplift loads of 0, $T_{u1}/3$ and $T_{u1}/2$, and a horizontal load of 500 N. The first zero-displacement points of these curves with similar shapes could be found at about 3D below the ground. It is noticed that the pre-applied uplift load has mainly reduced the horizontal displacement of pile body above that point. Specifically, with increasing uplift load, the displacement of this section has developed decreasing-increasing mode, yet little influence has been observed on the pile section below the first zero-displacement point.

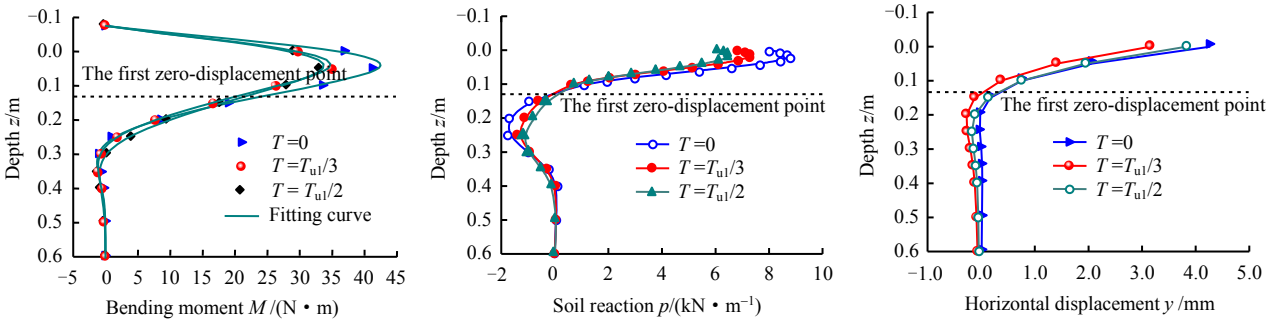

(a) Bending moment of pile body (b) Soil reaction around pile (c) Horizontal displacement of pile body

Fig. 5 Distribution of bending moment, soil pressure and horizontal displacement along pile at H=500 N

Hyperbola curves have been employed to fit p-y scatter points of the pile body at different depths. For example, Figure 6 gives regression results of single piles at 1D depth corresponding to the uplift loads of 0, $T_{u1}/3$ and $T_{u1}/2$. R^2 is greater than 0.99 and hence the regression quality is deemed good.

It is noted from the figure that the horizontal stiffness of the foundation is affected by the pre-applied uplift load. Substantially, at the same horizontal displacement, the soil reaction force of the pile subject to pure horizontal load is the largest, followed by the cases with T=$T_{u1}/3$ and T=$T_{u1}/2$ in sequence, demonstrating that increasing the pre-applied uplift load leads to the reduction of horizontal stiffness.

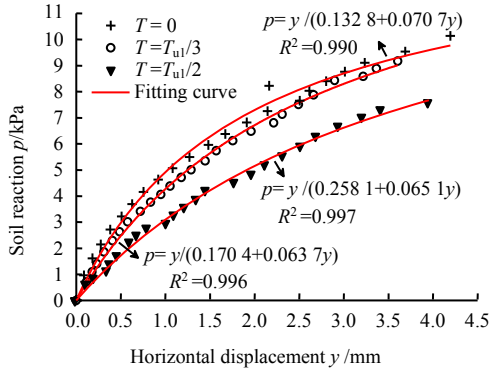

Fig. 6 p-y curves for 1D depth below ground surface

3.2 Bearing characteristics under uplift load

3.2.1 Load–vertical displacement curve

Figure 7 (a) illustrates the curves of uplift load (T) versus vertical displacement (v) of the pile top corresponding to the horizontal loads of 0, $H_{u1}/3$ and $H_{u1}/2$, and the upward direction is specified positive. The vertical displacement is hardly affected by pre-applied horizontal load when $T\leqslant$1 750N. When T further increases, the beneficial effect that the pre-applied horizontal load reduces v exhibited. This effect got enhanced when increasing the pre-applied horizontal load. Generally, each $T-v$ curve follows the trend of straight-curved-straight. Following the criteria introduced above, the uplift ultimate capacity of each pile corresponding to H=0, H= $H_{u1}/3$ and H= $H_{u1}/2$ was calculated as T_{u1}=2 460 N, T_{u2}= 2 740 N, T_{u3}=2 880 N, respectively. The last two magnitudes, i.e. T_{u2} and T_{u3}, have increased by 11.38% and 17.07%, respectively compared with T_{u1}, demonstrating that the pre-applied horizontal load improves the uplift ultimate bearing capacity of a single pile, and the effect is enhanced when increasing H.

Figure 7(b) shows curves of horizontal load (H) against displacement (v) of each test pile corresponding to uplift loads of 0, $T_{u1}/3$ and $T_{u1}/2$. For the pile under pure horizontal load, the vertical displacement v does not develop with horizontal loading due to the small deflection angle of the pile body at the early stage of loading. During the late stage of loading, however, negative displacement starts developing at an increasing rate because of the accumulation of deflection angle at pile top. For piles subject to combined load (T=$T_{u1}/3$ and T=$T_{u1}/2$), when H increases, both pile tops move upward firstly with a slowly linearly growing displacement. This upward displacement starts to decline once reaching the peak, and a higher changing rate is observed compared to that at the rising stage.

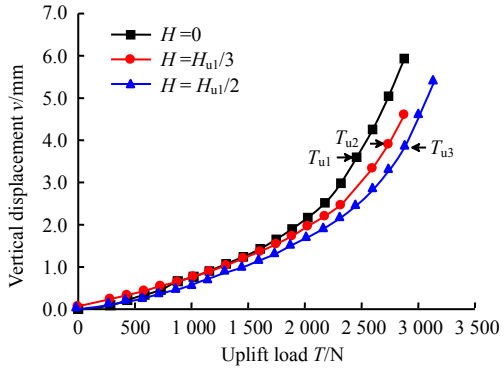

(a) Uplift load (T)– Vertical displacement (v) curve

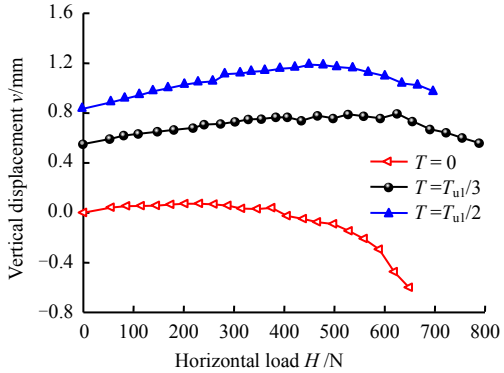

(b) Horizontal load (H)– Vertical displacement (v) curve

Fig. 7 Vertical deflection at pile head against different loads

3.2.2 Relative strain of pile body

The relative strain is defined as the difference between the strain measured at the current uplift load level and that measured before the first level is applied. The change rate of relative strain along the pile body reflects the friction resistance on both sides exactly. Figure 8 shows the relative strain distribution curves at both sides of the pile body corresponding to different pre-applied horizontal loads 0, $H_{u1}/3$ and $H_{u1}/2$. In comparison among these figures, the pre-applied horizontal loads ($H_{u1}/3$ and $H_{u1}/2$) only affects the relative strain and friction resistance on both sides of the pile within the distance of 10D below the ground, and the influenced range could be further divided into regions I and II. In region I, the change rate of relative strain in the front of piles under combined loads (H=$H_{u1}/3$ and H=$H_{u1}/2$) is higher than that of pure uplift pile (H =0), yet performs oppositely on the back side. It indicates that the friction resistance at pile front has been increased by stress expansion at this side in region I, while the friction resistance reduced at the back of pile due to stress release and decrease of contact area between pile and soil. Furthermore, the relative strain at the junction of region I and II in the front of the pile under combined loaded is significantly smaller than that under pure uplift load, yet the opposite result could be found on the back side. This is understandable as the additional bending moment M_τ produced by the unbalanced friction resistance of the front and back sides of the pile body in zone I is greater than the reverse additional bending moment M_Δ caused by the P-Δ effect, and consequently pure bending moment in the direction of M_τ is developed. As a result, the relative strain in the front of the combined loaded pile is smaller compared with the pure uplift pile, while the back is larger. When the uplift load T is small, the relative strain on the back side of pile in region I basically does not change along the depth, as it is mainly caused by the loss of friction resistance after the separation of the pile and soil. Regarding the increase of the uplift load, the relative strain of the back side in the same region develops positively along the depth, resulting from additional bending moment M_τ.

Because of opposite directions of pile body motion between region I and II, the change rate of relative strain on the back side of pile under combined load in region II is greater than that of pile under pure uplift load, while an opposite behavior can be observed at the front side.

3.2.3 Distribution of average friction resistance

Figure 9 presents distribution curves of average friction resistance of pile body under different uplift loads with pre-applied horizontal loads of 0, $H_{u1}/3$ and $H_{u1}/2$. It could be concluded that the average friction resistance of the pile shaft within the distance of 0.2 m (5D) under the ground has been significantly increased by the pre-applied horizontal load. For example, when T =1 750 N, the average friction resistance of the pile within the

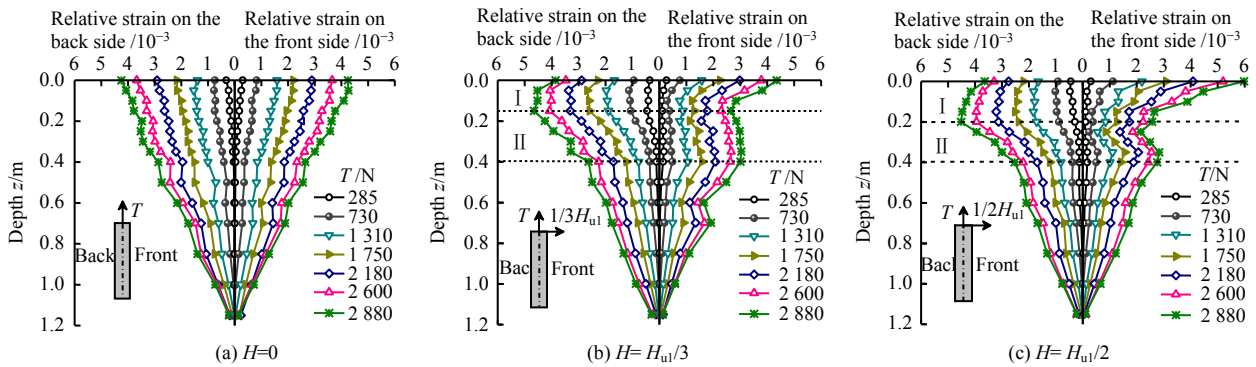

(a) H=0 (b) H= $H_{u1}/3$ (c) H= $H_{u1}/2$

Fig. 8 Relative strain distribution along pile on both sides

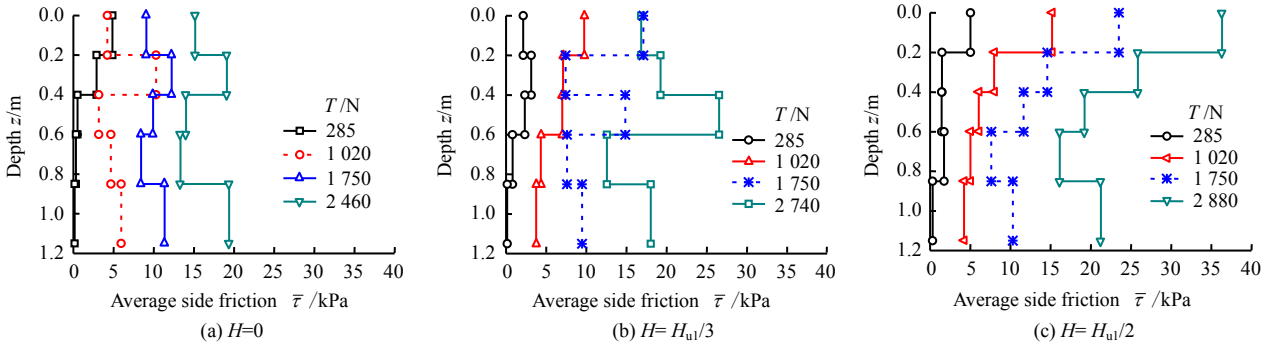

Fig. 9 Average side friction distribution along pile

distance of 0.2m has reached 9.09, 17.12 and 23.50 kPa corresponding to these three cases of 0, $H_{u1}/3$ and $H_{u1}/2$, respectively. The average friction resistance of the pile within the depth of 0.2–0.4 m significantly increases only when T is fairly large ($H_{u1}/2$). The friction resistance at the depth of 0.4–0.6 m in Fig. 9 (b) is obviously greater than that in other cases or the value shown in Fig. 9 (a) and Fig. 9 (c), and it has been explained as the abnormity of strain gauge at 0.6m in front of the pile. This problem can also be verified from Fig. 8 (b) where the relative strain at 0.6 m in front of the test pile with H=$H_{u1}/3$ has a sharp decrease.

4 Theoretical research

4.1 Influence of uplift load on horizontal bearing characteristics

The bearing characteristics of pile foundation depends on pile-soil interaction. The influence of pre-applied uplift load on this interaction mainly includes three aspects [22]:

(1) Second-order deflection effect ($P-\Delta$ effect). The horizontal load results in pile deflection, and then reverse additional bending moment M_Δ on the cross-section of the pile body at any depth s is produced as a result of the existing uplift load. The expression of M_Δ can be written as

$$M_\Delta = -T\cdot\Delta(s) \tag{9}$$

where $\Delta(s)$ is the horizontal displacement of the action point of uplift load relative to the center of the cross-section of the pile body at the depth of s.

(2) Friction effect. Different earth pressures on the front and back sides of the pile body have generated under combined loads, resulting in unbalanced friction resistance. The pressure difference produces additional bending moment M_τ on the pile body, contributed by the pile deflection deformation ($M_{\tau-\delta}$ part) and the pile diameter ($M_{\tau-r}$ part)[23], with both contributions having the same direction of the horizontal load. The earth pressure on the pile surface is non-uniformly distributed along the depth and the pile cross-section, and thus the magnitude of pile side friction resistance depends on the depth and its plane position. Neglecting the friction resistance on the stress releasing side, as shown in Fig.10, the additional bending moment $M_\tau(z-s)$ on the cross-section of the pile body at the depth of s induced by the friction resistance at any depth z ($0\leqslant z\leqslant s$) can be calculated as

$$M_\tau(z-s)=\int_{-\frac{\pi}{2}}^{\frac{\pi}{2}}\tau_v(z,\theta)(\delta+r\cos\theta)\mathrm{d}\theta\ (0\leqslant z\leqslant s) \tag{10}$$

where $\tau_v(z,\theta)$ is the vertical friction resistance at the point that lies at an angle of θ with respective to the loading direction on the z-depth cross-section; $\delta=\Delta(s)-\Delta(z)$ is the horizontal displacement of the cross-sections at the depth of s relative to that of z, and $\delta<\Delta(s)$; r is the pile radius. The additional bending moment M_τ developed by resultant friction forces above the depth s is

$$M_\tau=\int_0^s\int_{-\frac{\pi}{2}}^{\frac{\pi}{2}}\tau_v(z,\theta)\left(\delta+r\cdot\cos\theta\right)\mathrm{d}\theta\,\mathrm{d}z \tag{11}$$

where $\int_0^s\int_{-\frac{\pi}{2}}^{\frac{\pi}{2}}\tau_v(z,\theta)\cdot\delta\mathrm{d}\theta\mathrm{d}z$ is the moment caused by pile deflection deformation ($M_{\tau-\delta}$); and $\int_0^s\int_{-\frac{\pi}{2}}^{\frac{\pi}{2}}\tau_v(z,\theta)\cdot r\cos\theta\mathrm{d}\theta\mathrm{d}z$ refers to the bending moment contributed by pile diameter ($M_{\tau-r}$ part).

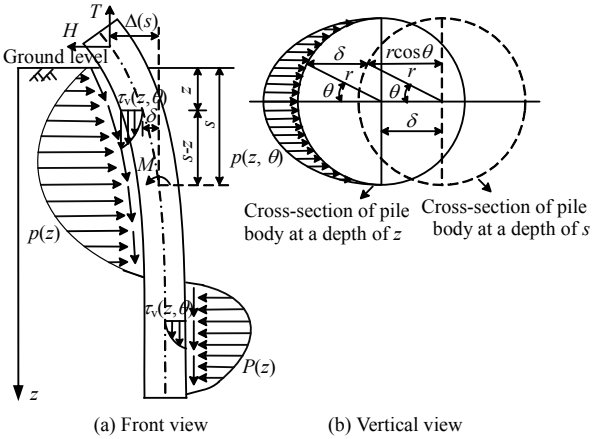

Fig. 10 Calculation schematic of additional bending moment caused by uplift loading

Under pure horizontal loading condition, in fact, the load is not perpendicular to the pile axis due to the

deflection of the pile body, which also leads to friction effect. However, the component of this load along the pile axis direction is too small to drive the sliding friction between the pile and soil. Therefore, the application of uplift load can increase $\tau_v(z,\theta)$, and cause greater friction effect. If the increment of frictional resistance caused by uplift load is $\tau'_v(z,\theta)$, then it leads to an increment of additional bending moment given as

$$M'_\tau = \int_0^s \int_{-\frac{\pi}{2}}^{\frac{\pi}{2}} \tau'_v(z,\theta)\left(\delta + r\cdot\cos\theta\right) \mathrm{d}\theta \,\mathrm{d}z \tag{12}$$

The bending moment M at any depth under combined loads could be expressed as

$$M = M_0 + M'_\tau - M_\Delta \tag{13}$$

where M_0 is the bending moment of pile body under pure horizontal load. Equation (13) implies that the influence of uplift load (T) on bending moment M is dominantly attributed by $M'_\tau - M_\Delta$. Regarding the pile under combined loads, the total vertical friction cannot be greater than the uplift load T, and $\delta < \Delta(s)$, which means the additional bending moment caused by pile deflection is greater than that of P–Δ effect $M_{\tau-\delta} < M_\Delta$ under the same lateral displacement. It has been found that only when the radius r exceeds a certain larger value of r', $M'_\tau - M_\Delta > 0$ takes place and the pre-applied uplift load enlarges bending moment M. However, for the pile with a smaller radius ($r < r'$) such as model piles in this study, it has been observed that the pre-applied uplift load leads to reduction of bending moment. Specifically, the unbalanced friction increases, while bending moment M decreases gradually with uplift load in this test.

(3) The increased friction at the pile-soil interface has an unloading effect on the surrounding soil [24]. Compared with the pile-soil system under pure horizontal load, the friction resistance on the pile-soil interface significantly increases with the uplift load at the pile top, reducing the vertical stress of the soil around the pile. Consequently, the foundation strength in terms of horizontal stiffness has been reduced. This effect also increases the horizontal displacement of the pile body under the same horizontal load, resulting in unfavorable impact on the bearing deformation behavior of the pile. Figure 6 shows that this stiffness weakening of the foundation has been enhanced under larger pre-applied uplift load T. Therefore, it can be concluded that static friction dominants vertical friction resistance between the pile and soil, the value of which increases with increasing uplift load. This conclusion is consistent with the results of Achmus et al [7].

In this test, the resultant effect of friction and $P-\Delta$ effect reduce the bending moment of the pile, which is beneficial in reducing the horizontal displacement of the pile body. Meanwhile, however, the unloading effect in the surrounding soil induced by the increased friction resistance at the pile-soil interface has weakened the horizontal stiffness of the foundation. Therefore, the horizontal displacement of the pile above the first zero-displacement point decreases at early stage but then increases with increasing uplift load under this comprehensive effect. For piles under combined loads, this displacement is always smaller than that of piles under pure horizontal load, and the corresponding horizontal ultimate bearing capacity increases at early stage and subsequently decreases with increasing uplift load.

4.2 Influence of horizontal load on uplift bearing characteristics

Shear failure with a cylindrical shape has occurred along the pile-soil interface of the pile under pure uplift load in this test, and the uplift ultimate bearing capacity T_u has been calculated by the following formula:

$$T_u = \pi D \int_0^L \mu K \gamma z + c' \mathrm{d}z \tag{14}$$

where μ is the pile-soil friction coefficient; K is the lateral earth pressure coefficient; γ is the effective unit weight of soil; c' is the pile–soil cohesion strength; and L is the length of the embedded pile section into the soil. The lateral earth pressure coefficient K is determined depending on the construction method. For ordinary pile, $K_0 = 1 - \sin\varphi$, and regarding partial-displacement pile and displacement pile, $K > K_0$. In this test, the compression between pile and soil has occurred during the process of soil compaction. Therefore, taking $K = K_0$ may underestimate the uplift bearing capacity in calculation. Instead, $K = \sqrt{K_p}$ has been adopted in this research, where K_p is the coefficient of Rankine passive earth pressure. The average friction resistance of the pile side within 5 cm distance under the ground has been considered to be fully provided by the pile-soil cohesion strength c'. Hence by calculating the average friction resistance within this section under the uplift ultimate load (2 460 N), this value was derived as $c' = 10.1$ kPa. Subsequently, the pile soil friction coefficient was calculated as $\mu = 0.362$, after substituting both values of K and c' into Eq. (14). The self-weight of the pile was considered during the analysis, and the uplift ultimate bearing capacity was determined as 2 400 N.

For piles subjected to combined loads (H=H_{u1}/3 and H=H_{u1}/2), the pre-applied horizontal load at pile top causes stress expansion on one side of the upper pile body, resulting in an increase in the average horizontal stress $\Delta\sigma_n$, and a stress release on the other side reducing horizontal stress by $-\Delta\sigma'_n$. The increasing horizontal displacement of the pile leads to the separation of pile's stress release side from the soil, resulting in the reduction in the pile-soil contact area. Generally, the influence of horizontal load H on the uplift bearing capacity of a single pile includes three parts: the increment of frictional

resistance caused by the increment of horizontal stress $\Delta\sigma_n$, the decrease of friction resistance caused by $-\Delta\sigma'_n$ on the other side and the loss of pile-soil cohesion strength. Therefore, the increase of uplift bearing capacity ΔT_u caused by horizontal load can be expressed as

$$\Delta T_u = \frac{\pi D}{2}\left(\int_0^h -c'\mathrm{d}z + \mu\int_0^L \Delta\sigma_n - \Delta\sigma'_n\mathrm{d}z\right) \tag{15}$$

where h is the length of pile−soil separation section.

Referring to the research of Mei et al. [25] on the displacement required for clay to develop active earth pressure, in this paper, an intermediate value of 0.007 L_1 (L_1 is the height of retaining wall) has been taken as the horizontal displacement for pile−soil separation. L_1 could be regarded as the depth corresponding to the first zero-displacement point of the pile body for flexible piles. As shown in Fig. 5 (c), a value of 120 mm has been adopted for L_1, which means the separation takes place as soon as the horizontal displacement of pile cross-section reaches 0.84 mm. In this research, considering the influence of uplift load T, horizontal displacement u =6 mm was taken and hence the depth of pile−soil separation h =103 mm was derived.

Neglecting the reduction in lateral earth pressure of the pile under horizontal loading caused by post-applied uplift load T, the increment of pure horizontal stress has been calculated by equivalently replacing the flexible pile with rigid one, and the relationship of length between equivalent rigid pile L_e and flexible pile L has been expressed as [26]

$$L_e / L = 2.1K_{rc}^{0.2} \leqslant 1 \tag{16}$$

where K_{rc} is the relative stiffness of the model pile, calculated by the following equation[27]

$$K_{rc} = EI / E_s L^4 \approx 2\times10^{-5} < 10^{-2}$$

where E_s is the horizontal modulus of soil at pile top derived from back analysis on horizontal displacement and rotation angle of the pile body at ground. Therefore, L_e=289 mm can be determined. The accumulated horizontal stress profile along the pile length is expressed as

$$\frac{\pi D}{2}\int_0^L \Delta\sigma_n - \Delta\sigma'_n\mathrm{d}z = \left(2.214 + 3.572\frac{e}{L_e}\right)H \tag{17}$$

$$\Delta T = \left(2.214 + 3.572\frac{e}{L_e}\right)\mu H - \frac{\pi}{2}DL_1c' \tag{18}$$

where e is the distance from the loading point to the ground (75 mm). The uplift ultimate bearing capacity T_{ui} of the pile under combined loads is

$$T_{ui} = T_{u1} + \Delta T \tag{19}$$

Table 2 has compared the calculation results against testing data of uplift ultimate bearing capacity of pile under combined loads. The results based on the theoretical analysis introduced above are slightly lower than the testing data, but the error is less than 6.0%, indicating good calculation accuracy.

Table 2 Comparison between predicted uplift ultimate uplifting bearing capacities and testing data

Horizontal load	Uplift ultimate bearing capacity /N		Error /%
	Test results	Predicted results	
$H_{u1}/3$	2 740	2 616	−4.53
$H_{u1}/2$	2 880	2 730	−5.21

5 Conclusions

(1) The horizontal ultimate bearing capacity of a single flexible pile can be improved under pre-applied load less than $T_{u1}/2$. Specifically, with the increase of uplift load, this capacity is enhanced at lower load level but then decreases under further uplift loading, while the maximum bending moment and the soil reaction force at the side of the pile are continuously decreasing. The horizontal displacement of the pile above the first zero-displacement point has also shown a similar trend of increasing and decreasing with uplift load, while the pile section below this point is basically not affected.

(2) The uplift ultimate bearing capacity of a flexible single pile can be improved via increasing friction resistance on pile-soil interface within the distance of 0−10D below the ground. This friction can be enhanced with horizontal load lower than $H_{u1}/2$. Especially when the horizontal load reaches $H_{u1}/2$, the corresponding uplift ultimate bearing capacity T_{u3} has increased by 17.3% compared to pure uplift load condition T_{u1}. This improvement on uplift ultimate bearing capacity could be noteworthy for the design work.

(3) Under pre-applied uplift load condition, little effect on the vertical displacement of the pile top induced from horizontal load has been observed. However, regarding the pile with pre-applied horizontal load, the horizontal displacement of the pile body on the ground increases significantly with increasing uplift load. Attention should be paid to the influence of the uplift load on horizontal stiffness of the foundation in practical design.

(4) The friction effect of the pile body under combined loads are of high relevance of the pile radius and roughness. When the pile diameter increases to a certain level, the resultant effect of $P-\Delta$ and friction may possibly increase the pile bending moment, yet further study is still required on the influence of pile radius.

References

[1] LIU Zu-de. Uplift pile foundation[J]. Ground Improvement, 1995, 6(4): 1−12.

[2] SHIN E C, DAS B M, PURI V K, et al. Ultimate uplift capacity of model rigid metal piles in clay[J]. Geotechnical

and Geological Engineering, 1993, 11(3): 203−215.

[3] YANG Ming-hui, YANG Xue-wen, ZHAO Ming-hua. Study of model experiments on uplift piles in clay under oblique loads[J]. Journal of Hunan University(Natural Sciences), 2016, 43(11): 13−19.

[4] RAMADAN M I, BUTT S D, POPESCU R. Offshore anchor piles under mooring forces: numerical modeling[J]. Canadian Geotechnical Journal, 2013, 50(2): 189−199.

[5] RAMADAN M I, BUTT S D, POPESCU R. Offshore anchor piles under mooring forces: Centrifuge modeling[J]. Canadian Geotechnical Journal, 2013, 50(4): 373−381.

[6] BHARDWAJ S, SINGH S K. Influence of load obliquity on pullout capacity of micropile in sand[J]. Indian Geotechnical Journal, 2015, 45(2): 200−208.

[7] ACHMUS M, THIEKEN K. On the behavior of piles in non-cohesive soil under combined horizontal and vertical loading[J]. Acta Geotechnica, 2010, 5(3): 199−210.

[8] MEYERHOF G G. The uplift capacity of foundations under oblique loads[J]. Canadian Geotechnical Journal, 1973, 10(1): 64−70.

[9] XU Jing-rong, HAO Chen-dong. Anti-floating design of a large-scale underground structure in high water level area[J]. Journal of Water Resources and Architectural Engineering, 2015, 13(5): 195−199.

[10] RAO S N, PRASAD Y V S N. Uplift behavior of pile anchors subjected to lateral cyclic loading[J]. Journal of Geotechnical Engineering, 1993, 119(4): 786−790.

[11] LUO Shao-feng, YANG Wen-xing. Static lateral loading tests of single pile combined uplift load with lateral load[J]. Geotechnical Investigation & Surveying, 2012, 40(6): 1−4.

[12] REDDY K M, AYOTHIRAMAN R. Experimental studies on behavior of single pile under combined uplift and lateral loading[J]. Journal of Geotechnical and Geoenviron-mental Engineering, 2015, 141(7): 04015030.

[13] SCHMERTMANN J H. Discussion of "experimental studies on behavior of single pile under combined uplift and lateral loading" by K. Madhusudan Reddy and R. Ayothiraman[J]. Journal of Geotechnical and Geoenvironmental Engineering, 2016, 142(8): 07016015.

[14] BHAVIK P, THAKARE S W. Performance of pile groups under combined uplift and lateral loading[J]. International Journal of Innovative Research in Science, Engineering and Technology, 2016, 5(6): 9219−9227.

[15] CAO Wei-ping, XIA Bing, ZHAO Min, et al. *p-y* curves of laterally loaded batter piles in sand and its application[J]. Chinese Journal of Rock Mechanics and Engineering, 2018, 37(3): 743−753.

[16] CHANDRASEKARAN S S, BOOMINATHAN A, DODAGOUDAR G R. Group interaction effects on laterally loaded piles in clay[J]. Journal of Geotechnical and Geoenvironmental Engineering, 2010, 136(4): 573−582.

[17] XU Guang-ming, ZHANG Wei-min. Study on particle size effect and boundary effect in centrifugal model[J]. Chinese Journal of Geotechnical Engineering, 1996, 18(3): 80−86.

[18] ZHAO Ming-hua, LI Wei-zhe, YANG Ming-hui, et al. A model test study on displacement of piles under inclined and eccentric loads in layered soils[J]. China Civil Engineering Journal, 2006, 39(12): 95−99.

[19] BHARDWAJ S, SINGH S K. Pile capacity under oblique loads–evaluation from load–displacement curves[J]. International Journal of Geotechnical Engineering, 2014, 9(4): 341−347.

[20] SINNREICH J, AYITHI A. Derivation of *p-y* curves from lateral pile load test instrument data[J]. Geotechnical Testing Journal, 2014, 37(6): 20130127.

[21] CHEN Xiang, SUN Jin-zhong, CAI Xin-bin. Horizontal static loading test and analyses of internal force and distortion on single pile[J]. Rock and Soil Mechanics, 2010, 31(3): 753−759.

[22] MU Lin-long, KANG Xing-yu, LI Wan. Analytical method for single pile under V-H-M combined loads in sand[J]. Chinese Journal of Geotechnical Engineering, 2017, 39(Suupl.2): 153−156.

[23] LI Hong-jiang, LIU Song-yu, TONG Li-yuan, et al. Method to analyze lateral bearing capacity of small deformation piles considering friction effect[J]. Chinese Journal of Rock Mechanics and Engineering, 2018, 37(1): 230−238.

[24] WANG Tie-hang, JIN Xin, LUO Yang, et al. A method for evaluation of loess collapse potential of unloading[J]. Rock and Soil Mechanics, 2019, 40(4): 1281−1290.

[25] MEI Guo-xiong, ZAI Jin-min. Rankine earth pressure model considering deformation[J]. Chinese Journal of Rock Mechanics and Engineering, 2001, 20(6): 851−853.

[26] MEYERHOF G G, SASTRY V V R N, YALCIN A S. Lateral resistance and deflection of flexible piles[J]. Canadian Geotechnical Journal, 1988, 25(3): 511−522.

[27] POULOS H G. DAVIS E H. Pile foundation analysis and design[M]. New York: John Wiley and Sons, 1980.